Three manganese complexes of anionic N_4-donor Schiff-base macrocycles: monomeric Mn(II) and Mn(III), and dimeric Mn(IV)

Rajni K. Wilson,[A] *Sébastien Dhers,*[A] *Stephen Sproules,*[B] *Eric J. L. McInnes*[C] *and Sally Brooker*[A D]

[A] Department of Chemistry and MacDiarmid Institute for Advanced Materials and Nanotechnology, University of Otago, PO Box 56, Dunedin 9054, New Zealand.

[B] WestCHEM, School of Chemistry, University of Glasgow, Glasgow G12 8QQ, UK

[C] School of Chemistry and Photon Science Institute, The University of Manchester, Oxford Road, Manchester M13 9PL, UK

[D] Corresponding author. Email: sbrooker@chemistry.otago.ac.nz.

Dedicated to Emeritus Professor Richard Robson (University of Melbourne), an outstandingly innovative and intelligent scientist, and a true gentleman, whose seminal research contributions to macrocyclic chemistry and metal organic frameworks are internationally renowned.

Three manganese macrocyclic complexes of two anionic N_4-donor [1+1] Schiff-base macrocycles that differ in ring size (14 vs 16 membered), H$\mathbf{L}^{\mathbf{Et}}$ and H$\mathbf{L}^{\mathbf{Pr}}$ (obtained from condensation of diphenylamine-2,2'-dicarboxaldehyde and either diethylenetriamine or dipropylenetriamine), are reported. Specifically, a pair of monomeric complexes $Mn^{II}\mathbf{L}^{\mathbf{Et}}(NCS)(H_2O)$ and $[Mn^{III}\mathbf{L}^{\mathbf{Pr}}(NCS)_2]\bullet 0.5H_2O$, plus a dimeric complex $[Mn^{IV}{}_2\mathbf{L}^{\mathbf{Et}}{}_2(O)_2](ClO_4)_2\bullet 3DMF$ have been synthesised and characterised. Single crystal structure determinations on $[Mn^{III}\mathbf{L}^{\mathbf{Pr}}(NCS)_2]\bullet 0.5H_2O$ and $[Mn^{IV}{}_2\mathbf{L}^{\mathbf{Et}}{}_2(O)_2](ClO_4)_2\bullet 3DMF$ revealed octahedral manganese centres in both cases: N_6-coordinated Jahn-Teller distorted Mn(III) in the former and a pair of N_4O_2-coordinated Mn(IV) in the latter. UV-vis, IR and EPR spectroscopy as well as magnetic measurements are reported. These macrocyclic complexes feature a simple and original design, and could find future uses as models for manganese catalase or as building blocks for the assembly of larger supramolecular architectures.

Manuscript received: xx April 2019.
Manuscript accepted: xx XXXX 2019.
Published online: xx XXXX 2019.

Introduction

Macrocycles are polydentate ligands with the donor atoms either incorporated in, or less commonly attached to, a cyclic backbone.[1] Porphyrins, chlorins and corrins are classes of naturally occurring, highly conjugated, tetrapyrrolic, N_4-donor macrocycles.[2-4] The complexes of all of these porphyrin-like N_4-donor macrocycles are biologically important molecules, exhibiting a variety of critical functions, such as oxygen transport (haemoglobin: iron complex of porphyrin), photosynthesis (chlorophylls: magnesium complexes of chlorins) and formation of blood in our body (vitamin B_{12}: cobalt complex of corrin).[3-5]

Manganese ions are also involved in the active sites of a number of metalloenzymes that perform biological redox reactions.[3, 6] In these natural systems, the manganese ions cycle through various different oxidation states during the catalytic cycle. Manganese catalases, which are responsible for the disproportionation of two molecules of hydrogen peroxide into water and oxygen, possess a dinuclear, O-bridged, manganese active site which cycles between $Mn(II)_2$ and Mn(II)-Mn(III) during the catalytic cycle.[7, 8] This, and interest in the Mn_4Ca cluster in photosystem II which undergoes a cycle of four oxidation steps in order to catalyse the oxidation of two molecules of water into oxygen and protons,[9-17] has led to di- and poly-nuclear manganese complexes in a range of oxidation states being studied as models for the active sites of these systems.[18-26]

Macrocycles are a very useful ligand type for producing models of such biological active sites, not least as they provide a lot of control over the coordination site of the bound metal ion(s).[27] Interest in Schiff-base macrocycles in particular has remained high, and remains a particular strength in Australasia ever since the pioneering contributions to this field by Neil Curtis[28, 29] and Richard Robson.[30] In this paper we describe the synthesis and characterisation of three manganese complexes of a pair of N_4-donor [1+1] Schiff base macrocycles, differing only in ring size, developed previously in our group,[31-33] as we built on studies, published a decade earlier, by David Black.[34] Whilst these anionic macrocycles, $(\mathbf{L}^{\mathbf{Et}})^-$ and $(\mathbf{L}^{\mathbf{Pr}})^-$, share some similarities with the naturally occurring porphyrin and porphyrin-like macrocycles (above), in that they all provide an N_4-donor environment, herein they exhibit a significant difference: greater flexibility of coordination mode, as might be

expected given the far lower extent of conjugation. The resulting manganese complexes, $Mn^{II}\mathbf{L}^{Et}(NCS)(H_2O)$, $[Mn^{III}\mathbf{L}^{Pr}(NCS)_2]\bullet 0.5H_2O$ and $[Mn^{IV}{}_2\mathbf{L}^{Et}{}_2(O)_2](ClO_4)_2\bullet 3DMF$, vary in oxidation states (+II, +III or +IV), ligand binding modes (meridional or facial), and nuclearity (monomer or dimer).

Results and Discussion

The pair of monomeric complexes, $Mn^{II}\mathbf{L}^{Et}(NCS)(H_2O)$ and $[Mn^{III}\mathbf{L}^{Pr}(NCS)_2]\bullet 0.5H_2O$, was synthesised in good yields (50 and 78%) by the addition of one equivalent of $Mn^{II}(py)_4(SCN)_2$, under an inert atmosphere, to a suspension of the appropriate macrocycle in dry MeOH (Scheme 1). Upon addition of the metal salt the suspension immediately clarified and changed to a pale orange colour. Note that in both cases the pyridine present in the manganese thiocyanate reagent, $Mn^{II}(py)_4(SCN)_2$, is expected to have deprotonated the macrocycle.

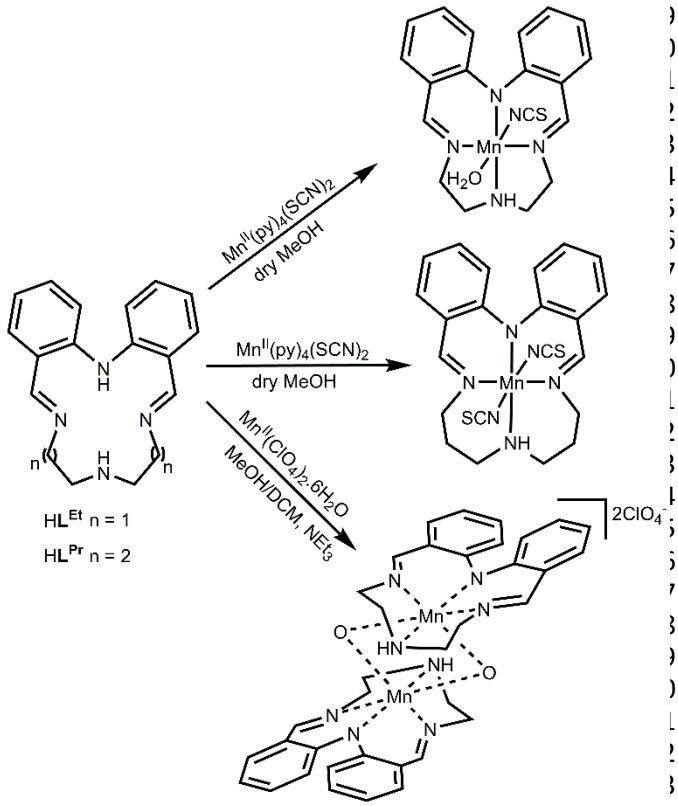

Scheme 1. The synthetic route to the manganese Schiff-base macrocyclic complexes reported herein: top $Mn^{II}\mathbf{L}^{Et}(NCS)(H_2O)$, middle $[Mn^{III}\mathbf{L}^{Pr}(NCS)_2]\bullet 0.5H_2O$, bottom $[Mn^{IV}{}_2\mathbf{L}^{Et}{}_2(O)_2](ClO_4)_2\bullet 3DMF$.

After stirring under argon for 2 hours, the colour slowly changed to dark brown for $Mn^{II}\mathbf{L}^{Et}(NCS)(H_2O)$. In the case of $[Mn^{III}\mathbf{L}^{Pr}(NCS)_2]\bullet 0.5H_2O$, the reaction solution was opened up to air after stirring during 4 hours under Ar, which resulted in an immediate colour change from pale orange to dark brown. After exposure to air for 3 hours with no obvious further colour change, the $H\mathbf{L}^{Et}$ reaction solution was vapour diffused with diethyl ether, in air, giving $Mn^{II}\mathbf{L}^{Et}(NCS)(H_2O)$ as a brown solid. In the case of $[Mn^{III}\mathbf{L}^{Pr}(NCS)_2]\bullet 0.5H_2O$, a longer period of exposure to air, 7 days was found to be optimal to obtain the pure manganese(III) complex, which conveniently precipitates out as a red solid. X-ray quality dark red blocks of $[Mn^{III}\mathbf{L}^{Pr}(NCS)_2]$ were obtained by diethyl ether vapour diffusion into a MeOH solution of the reaction solution in air. An attempted synthesis of the manganese(III) complex of the $(\mathbf{L}^{Et})^-$ macrocycle resulted in the manganese(II) complex.

The third complex was formed by complexation of $H\mathbf{L}^{Et}$ with $Mn(ClO_4)_2\bullet 6H_2O$ and one equivalent of base (NEt_3) in air, in a 1:1 mixture of dichloromethane and methanol, followed by diethyl ether vapour diffusion into the dark brown solution to give a dark brown solid. Diethyl ether vapour diffusion into a DMF solution of the sample, in air, gave a dark brown powder along with dark brown needles of $[Mn^{IV}{}_2\mathbf{L}^{Et}{}_2(O)_2](ClO_4)_2\bullet 3DMF$ suitable for an X-ray structure determination. The tentative assignment of the manganese(IV) oxidation state is based on the magnetic moment data and the structure determination (see below).

The positive ion electrospray mass spectra of $Mn^{II}\mathbf{L}^{Et}(NCS)(H_2O)$, $[Mn^{III}\mathbf{L}^{Pr}(NCS)_2]\bullet 0.5H_2O$ and the crystals of $[Mn^{IV}{}_2\mathbf{L}^{Et}{}_2(O)_2](ClO_4)_2\bullet 3DMF$ show a common peak, the fragment $[Mn(\mathbf{L}^{Et/Pr})\text{-}H]^+$, which is associated with the loss of an additional proton and the perchlorate or isothiocyanate co-ligand. Importantly, the $Mn(IV)_2$ dimer also shows a peak corresponding to a $[Mn_2\mathbf{L}^{Et}{}_2(O)_2(ClO_4)]^+$ dimer fragment.

The infrared spectra of the three manganese complexes had imine stretches in the range 1611-1628 cm^{-1}. In the $(\mathbf{L}^{Et})^-$ complexes the imine stretches (1624, 1628 cm^{-1}) occurred at slightly lower energies than in the metal-free macrocycle $H\mathbf{L}^{Et}$ (1629 cm^{-1}) whereas in the $(\mathbf{L}^{Pr})^-$ complex the imine stretch (1611 cm^{-1}) was at a significantly lower energy than in crude metal-free $H\mathbf{L}^{Pr}$ macrocycle (1628 cm^{-1}), as was observed in previously reported complexes of $(\mathbf{L}^{Pr})^-$.[32] The ν(CN) stretch of the isothiocyanate ions in $Mn^{II}\mathbf{L}^{Et}(NCS)(H_2O)$ and $[Mn^{III}\mathbf{L}^{Pr}(NCS)_2]\bullet 0.5H_2O$ is observed at 2050 and 2039 cm^{-1}, respectively, and is consistent with terminal N-bound ligand (literature range $\geq$ 2050 cm^{-1}),[35] which was subsequently confirmed by X-ray crystallography (see below). The Mn(IV) dimer showed two bands at 1074 cm^{-1} and 621 cm^{-1}, confirming the presence of the perchlorate anion.

The room temperature magnetic moment of 6.07 μ_B $Mn^{II}\mathbf{L}^{Et}(NCS)(H_2O)$ confirms a high-spin Mn(II) $S = {}^5/_2$ central ion. Its fluid solution EPR spectrum recorded at X-band exhibited the characteristic six-lines from coupling of the electron spin to the ^{55}Mn ($I = {}^5/_2$, 100% natural abundance) nucleus (Figure S1). Simulation yielded $g_{iso} = 2.0026$ and a hyperfine coupling constant of $A_{iso} = 89 \times 10^{-4}$ cm^{-1} typical for Mn(II). The Mn(III) ion in $[Mn^{III}\mathbf{L}^{Pr}(NCS)_2]\bullet 0.5H_2O$ is high-spin as denoted by its temperature independent μ_{eff} value of 4.91 μ_B (50–300 K) for an $S = 2$ ground state (Figure S2). Below 50 K, μ_{eff} decreases due to the influence of zero-field splitting. The susceptibility has been successfully modelled with a sizeable $|D| = 6.5$ cm^{-1} at near full rhombicity, $E/D = 0.029$. These parameters are consistent with Mn(III) $S = 2$ in such a ligand field, and with being EPR silent at X-band.[36-38] Full variable temperature (VT) measurement conducted in the temperature range 2–300 K for $[Mn^{IV}{}_2\mathbf{L}^{Et}{}_2(O)_2](ClO_4)_2\bullet 3DMF$ (Figure S3) gave a μ_{eff} value of 3.91 μ_B per Mn, consistent with 3 upe and hence Mn(IV). This μ_{eff} value drops only very slowly as the temperature is reduced, to a value of 2.74 μ_B, before dropping

rapidly thereafter. This profile is consistent with weak antiferromagnetic coupling.

X-ray Crystal Structures

Crystal structure determinations were carried out on $[Mn^{III}\mathbf{L}^{Pr}(NCS)_2]$ and $[Mn^{IV}_2\mathbf{L}^{Et}_2(O)_2](ClO_4)_2$•3DMF. Examination of these structures revealed that $[Mn^{III}\mathbf{L}^{Pr}(NCS)_2]$ is mononuclear with the manganese(III) ion in a Jahn-Teller distorted octahedral N_6-donor environment whereas $[Mn^{IV}_2\mathbf{L}^{Et}_2(O)_2](ClO_4)_2$•3DMF is dinuclear with the manganese(IV) ions also in an octahedral geometry.

Dark red blocks of $[Mn^{III}\mathbf{L}^{Pr}(NCS)_2]$ were obtained by diethyl ether vapour diffusion into a MeOH solution of the sample and the crystal structure determined (Figure 1).

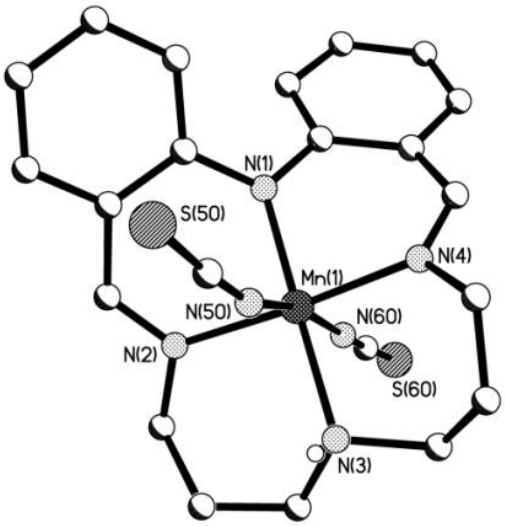

Figure 1. Perspective view of one of the two independent molecules of $[Mn^{III}\mathbf{L}^{Pr}(NCS)_2]$. Non acidic hydrogen atoms omitted for clarity.

Table 1. Selected bond lengths (Å), angles (°) and other parameters in the two independent molecules of $[Mn^{III}\mathbf{L}^{Pr}(NCS)_2]$.

Bond Length (Å)	
Mn–N_{dpa}: Mn(1)–N(1) / Mn(2)–N(6)	1.922(7), 1.913(7)
Mn–N_{imine}: Mn(1)–N(2) / Mn(2)–N(7)	2.031(7), 2.020(8)
Mn–N_{imine}: Mn(1)–N(3) / Mn(2)–N(8)	2.087(7), 2.101(8)
Mn–N_{imine}: Mn(1)–N(4) / Mn(2)–N(9)	2.015(7), 2.003(8)
Mn–N_{NCS}: Mn(1)-N(50)/Mn(2)–N(70)	2.217(7), 2.223(9)
Mn–N_{NCS}: Mn(1)–N(60)/Mn(2)–N(80)	2.203(7), 2.230(9)
Bond Angle (°)	
N(1)–Mn(1)–N(2) / N(6)–Mn(2)–N(9)	88.5(3), 89.0(3)
N(1)–Mn(1)–N(4) / N(6)–Mn(2)–N(7)	88.0(3), 88.4(3)
N(3)–Mn(1)–N(2) / N(8)–Mn(2)–N(7)	92.4(3), 91.2(3)
N(3)–Mn(1)–N(4) / N(8)–Mn(2)–N(9)	91.0(3), 91.4(3)
N(1)–Mn(1)–N(3) / N(6)–Mn(2)–N(8)	178.7(3), 178.8(3)
N(2)–Mn(1)–N(4) / N(9)–Mn(2)–N(7)	176.0(3), 177.4(3)
Phenyl rings twist (°)	62.48, 60.55
***cis* N–Mn–N angles (°)**	88.0-92.4, 88.4-91.4
***trans* N–Mn–N angles (°)**	176.0-178.7, 177.4-178.8
Average Mn–N distance (Å)	2.014, 2.009

The complex crystallises in the monoclinic space group $P2_1/n$. The monoanionic tetradentate macrocyclic ligand is bound to the equatorial plane of the metal centre through all four nitrogen atoms (one amine, one deprotonated amine and two imine nitrogen donors). In addition to the macrocycle, two axially coordinated (*trans*) isothiocyanate anions are also bound to the manganese(III) centre, forming an N_6 coordination environment. There are two entire $[Mn^{III}\mathbf{L}^{Pr}(NCS)_2]$ complexes in the asymmetric unit. The Mn(2) complex has no disorder whereas in the Mn(1) complex both CS atoms of the NCS^- anions and the four alkyl carbon atoms adjacent to the N(3) atom and the NH proton in the central part of the dipropylene triamine alkyl chain are disordered over two sites (occupancy of 0.75:0.25).

The shortest Mn–N bond distance involves the deprotonated diphenylamine nitrogen atom, Mn–N_{dpa} [1.922(7), 1.913(7) Å], whereas the longest is the Mn–N_{amine} bond [2.087(7), 2.101(8) Å]. The four crystallographically independent Mn–N_{imine} bond lengths are equivalent within experimental error and are of intermediate lengths (average 2.017 Å; Table 1).

A few dark brown needles of $[Mn^{IV}_2\mathbf{L}^{Et}_2(O)_2](ClO_4)_2$•3DMF were obtained by diethyl ether vapour diffusion into a DMF solution of the sample, in air, and the crystal structure determined (Figure 2 and Table 2). The complex crystallises in the monoclinic space group $P2_1/n$ with the entire complex in the asymmetric unit.

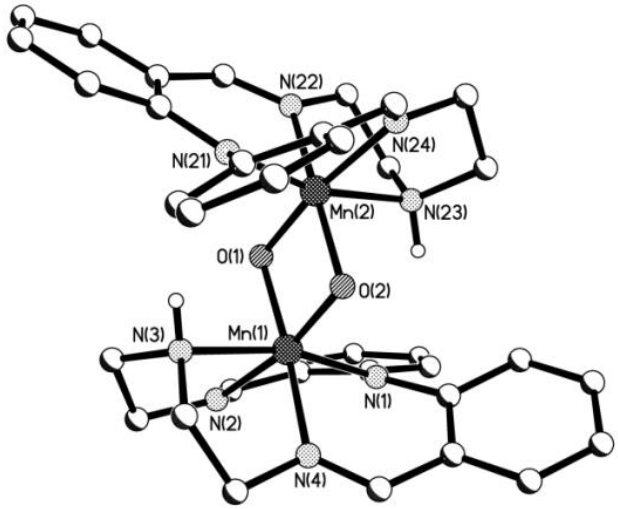

Figure 2. Perspective view of the cation of $[Mn^{IV}_2\mathbf{L}^{Et}_2(O)_2](ClO_4)_2$•3DMF. Hydrogen atoms, ClO_4^- anion and solvent of crystallisation omitted for clarity.

The geometry around each manganese centre is approximately octahedral, the ligating atoms being two *cis* oxo bridges and the four nitrogen atoms (one amine, one deprotonated amine and two imine nitrogen donors) from the $(\mathbf{L}^{Et})^-$ macrocycle. This is the *first observation of this tetradentate macrocycle binding in a capping not equatorial*, mode (and hence the co-ligands occupying *cis* sites): all previous structurally characterised complexes feature an equatorial binding mode (with the co-ligand in *trans* sites). This 14-membered anionic N_4-donor macrocycle has similarities to the 16-membered porphyrins, but this binding mode highlights a key difference: significantly

greater flexibility (due to much less conjugation) which enables the capping binding mode observed here.

Table 2. Comparison of selected bond lengths (Å), angles (°) and other parameters for $[Mn^{IV}_2\mathbf{L^{Et}}_2(O)_2](ClO_4)_2$•3DMF.

Bond Length (Å)			
Mn(1)–O(1)	1.811(2)	Mn(2)–O(1)	1.810(3)
Mn(1)–O(2)	1.819(3)	Mn(2)–O(2)	1.826(2)
Mn(1)–N(1)	1.978(3)	Mn(2)–N(21)	1.963(3)
Mn(1)–N(2)	2.004(3)	Mn(2)–N(22)	1.990(3)
Mn(1)–N(3)	2.076(3)	Mn(2)–N(23)	2.069(3)
Mn(1)–N(4)	2.010(3)	Mn(2)–N(24)	2.013(3)
Mn(1)···Mn(2)	2.708(10)		
Bond Angle (°)			
N(4)–Mn(1)–N(2)	94.0(13)	N(24)–Mn(2)–N(22)	93.7(13)
N(4)–Mn(1)–N(1)	87.8(13)	N(24)–Mn(2)–N(21)	87.6(14)
N(2)–Mn(1)–N(1)	89.8(13)	N(22)–Mn(2)–N(21)	91.1(13)
N(4)–Mn(1)–N(3)	81.7(12)	N(24)–Mn(2)–N(23)	80.9(13)
N(2)–Mn(1)–N(3)	81.0(13)	N(22)–Mn(2)–N(23)	80.9(13)
N(1)–Mn(1)–N(3)	165.5(12)	N(21)–Mn(2)–N(23)	165.5(13)
O(1)–Mn(1)–O(2)	83.7(11)	O(1)–Mn(2)–O(2)	83.5(11)
Mn(1)–O(2)–Mn(2)	95.9(12)	Mn(2)–O(1)–Mn(1)	96.8(12)
Phenyl rings twist (°)		37.85, 51.96	
Average Mn-N distance (Å)		2.017, 2.009	
Average Mn-O distance (Å)		1.815, 1.818	

The assignment of the single atom bridges as μ-oxo rather than μ-hydroxo, hence also the manganese oxidation states as +IV not +III was made only after careful consideration of the manganese coordination sphere, hydrogen bonding to another molecule and CSD searches. No evidence of a proton was found near either oxo atom in the difference maps.

To further probe the assignment of manganese oxidation states in $[Mn^{IV}_2\mathbf{L^{Et}}_2(O)_2](ClO_4)_2$•3DMF, a comparison with related structures was conducted. A search of the CSD (version 5.39) for N_4-coordinated, bis-O(any type) bridged, dimanganese complexes resulted in 104 hits, of which only 74 involved bis-oxo bridged complexes (the others mostly involved phenolate O bridging). Narrowing the search to those structures where the oxidation states are clearly entered in the CSD as 'manganese(X)' where X is II, III or IV, the manganese oxidation state combinations identified include 10 examples of Mn^{III}_2, 27 of $Mn^{III}Mn^{IV}$ and 5[refs 39-43] of Mn^{IV}.

The average Mn–O [1.815(3), 1.819(2) Å] and Mn-N distances [2.017, 2.009 Å] in $[Mn^{IV}_2\mathbf{L^{Et}}_2(O)_2](ClO_4)_2$•3DMF fall in the range for Mn^{IV}–O [1.772-1.829 (1.806) Å] and at the lower end of the range for Mn^{IV}–N [1.995-2.174 (2.077) Å] for literature bis(μ-oxo)-Mn^{IV}_2 complexes. The Mn–O–Mn angles [96.8(1), 96.0(1)°] also fall in the range observed for related bis-oxo-Mn^{IV}_2 complexes [95.1-101.4 (98.01)°], but not in the range for bis-oxo-Mn^{III}_2 complexes [92.1-94.8 (93.5)°]. The Mn···Mn separation of 2.708(10) Å falls within the literature range for bis(μ-oxo)Mn^{IV}_2 complexes [2.671-2.748 (2.724) Å], but also falls close to those reported for bis(μ-oxo)Mn^{III}_2 complexes [2.676-2.699 (2.689)Å].

A more detailed comparison of some of the key coordination sphere parameters in the present complex with those of three typical examples of structures selected from the CSD hits, in each of the three possible oxidation state combinations, Mn^{III}_2, localised $Mn^{III}Mn^{IV}$ and Mn^{IV}_2, is presented in Table 3.[39, 44, 45] For ease of comparison we have defined the equatorial plane as comprising both oxo groups and the two nitrogen donors in the same plane (N2, N4; N22, N24; Figure 2), with the axial direction comprising the remaining two nitrogen donors (N1, N3; N21, N23; Figure 2). In $[Mn^{IV}_2\mathbf{L^{Et}}_2(O)_2](ClO_4)_2$•3DMF the average axial Mn–N bond length (2.022 Å) is only slightly longer than the average equatorial bond length (2.004 Å), and both values are comparable to those in the bis(μ-oxo)dimanganese(IV) complex presented in Table 3, consistent with the oxidation state being Mn^{IV}_2. No Jahn-Teller distortion is observed, unlike in the Mn^{III}_2 complex bis(μ-oxo)bis[*N*,*N*′-bis((6-methylpyrid-2-yl)methyl)-ethane-1,2-diamine]dimanganese(III) perchlorate (Table 3),[44] so it is unlikely to be a Mn^{III}_2 or a localised $Mn^{III}Mn^{IV}$ complex. The Mn-N distances also indicate that the bridging oxo groups do not induce a *trans* effect on the equatorial nitrogen atoms, something which has been seen in some other bis(μ-oxo)-Mn^{IV}_2 complexes with $Mn–N_{equatorial} >> Mn–N_{axial}$.

In summary, the comparisons of Mn···Mn separation, average Mn–O and Mn-N distances, and Mn–O–Mn angles in $[Mn^{IV}_2\mathbf{L^{Et}}_2(O)_2](ClO_4)_2$•3DMF with other complexes (Table 3) do not allow a definitive assignment of oxidation state, but overall it is most likely to be in the Mn^{IV}_2 oxidation state.

Table 3. Selected distances (Å) for one 'typical' example of a structurally characterised bis(μ-oxo)dimanganese complex in each of the three oxidation state combinations, Mn^{III}_2, localised $Mn^{III}Mn^{IV}$ and Mn^{IV}_2, along with $[Mn^{IV}_2\mathbf{L^{Et}}_2(O)_2](ClO_4)_2$•3DMF.

Complex (CCDC code)	Mn···Mn	Mn–O	$Mn–N_{ax}$	$Mn–N_{eq}$	Mn–O–Mn	Ref.
$\mathbf{Mn^{III}_2}$ (KAWLID)	2.676(3)	Mn^{III} 1.814-1.863	Mn^{III} 2.406-2.468	Mn^{III} 2.099-2.121	92.1(4)-94.5(4)	[44]
$\mathbf{Mn^{III}Mn^{IV}}$ (SEJXUA)	2.741(1)	Mn^{III} 1.854-1.867 Mn^{IV} 1.786-1.791	Mn^{III} 2.336-2.362 Mn^{IV} 2.049-2.051	Mn^{III} 2.116-2.129 Mn^{IV} 2.111-2.115	97.7	[45]
$\mathbf{Mn^{IV}_2}$ (FEBKOM)	2.748(2)	Mn^{IV} 1.797-1.805	Mn^{IV} 1.999-2.020	Mn^{IV} 2.069-2.087	99.5(2)	[39]
$\mathbf{[Mn^{IV}_2L^{Et}_2(O)_2](ClO_4)_2}$• **3DMF**	2.708(10)	1.810-1.826	1.963-2.076	1.990-2.013	96.0(1)-96.8(1)	this work

Conclusions

Three manganese complexes, $Mn^{II}\mathbf{L}^{Et}(NCS)(H_2O)$, $[Mn^{III}\mathbf{L}^{Pr}(NCS)_2]\bullet 0.5H_2O$ and $[Mn^{IV}{}_2\mathbf{L}^{Et}{}_2(O)_2](ClO_4)_2\bullet 3DMF$, were prepared by deprotonation and metallation of the respective metal-free Schiff-base macrocycles, $H\mathbf{L}^{Et}$ and crude $H\mathbf{L}^{Pr}$. These anionic N_4-donor macrocycles have similarities with the anionic N_4-donor porphyrins, but also significant differences: herein their far greater flexibility, due to a much lower degree of conjugation, is demonstrated in the binding modes adopted: either meridional (equatorial square plane; *trans* co-ligands), or facial (capping; *cis* co-ligands). Also reported here are the first examples of these diphenylamine-2,2′-dicarboxaldehyde-based macrocycles facilitating access to 3d complexes in a wider range of oxidation states, +II, +III and +IV: all previous complexes having been isolated only in the +II oxidation state. The mononuclear complexes produced are of interest as building blocks for larger supramolecular architectures. Our current efforts are focussed on refining the macrocycle design further, in particular aiming to increase the denticity and to include surface-anchoring groups.

Experimental

Magnetic data for $Mn^{II}L^{Et}(NCS)(H_2O)$ was recorded at 300 K using a Quantum Design Physical Property Measurement System (PPMS) equipped with a vibrating sample mount with an applied field of 1 T. Variable temperature (2 – 300 K) magnetic susceptibility data for $[Mn^{III}L^{Pr}(NCS)_2]\bullet 0.5H_2O$ were recorded in a 1 T magnetic field on a SQUID magnetometer (MPMS, Quantum Design). All magnetic data were corrected for diamagnetic contributions using Pascal's constants. X-band EPR data were collected on a Bruker EMX Micro spectrometer equipped with a 'premium-X' microwave bridge and simulationed using Xsophe.[46] Elemental analyses were carried out by the Campbell Microanalytical Laboratory at the University of Otago.

MeOH and DMF were HPLC grade, whereas DCM was reagent grade and used without purification. $Mn^{II}(py)_4(SCN)_2$ [ref35] and the $H\mathbf{L}^{Et}$ macrocycle[31] were prepared as previously reported, but in the case of the $H\mathbf{L}^{Pr}$ macrocycle, rather than using the literature synthesis,[32] a crude sample of macrocycle was instead prepared without added acid (details below) and utilised without further purification.

$Mn^{II}\mathbf{L}^{Et}(NCS)(H_2O)$: Under an Ar atmosphere, to a bright yellow suspension of the macrocycle $H\mathbf{L}^{Et}$ (45.1 mg, 0.154 mmol) in methanol (30 mL) was added $Mn^{II}(py)_4(SCN)_2$ (75.3 mg, 0.154 mmol) as a solid, resulting in an pale orange coloured solution. After stirring under Ar for 2 hours, the colour slowly changed to dark brown. The solution was stirred at RT overnight and then exposed to air for 7 hours. The dark brown solution was concentrated to 20 mL under reduced pressure and finally subjected to diethyl ether vapour diffusion in air. The resulting brown solid was collected by filtration and dried *in vacuo* (33 mg, 50%). (Found: C, 53.57; H, 4.76; N, 16.33; S, 8.02%. Calc. for $[C_{19}H_{19}N_5SMn\bullet H_2O]$ (422.41 g mol^{-1}): C, 54.03; H, 5.01; N, 16.58; S, 7.59%). IR (ATR): ν/cm^{-1} = 3061, 2864, 2050, 1624, 1598, 1527, 1483, 1454, 1434, 1398, 1289, 1194, 1156, 1039, 972, 857, 750, 622, 535, 473. ESI(+) MS (*m*/*z*) (MeCN): $[Mn^{II}\mathbf{L}^{Et}\text{-}H]^+$ expected 345.0892, found 345.0906. μ_{eff} (PPMS at 300 K) = 6.07 μ_B. UV-vis (DMF): λ_{max}/nm (ε/dm^3 mol^{-1} cm^{-1}) = 343 (56904), 454 (2428). Λ_m (MeCN) = 53 Ω^{-1} cm^2 mol^{-1}.

$[Mn^{III}\mathbf{L}^{Pr}(NCS)_2]\bullet 0.5H_2O$: Under an Ar atmosphere, to a bright yellow suspension of the crude macrocycle $H\mathbf{L}^{Pr}$ (151.4 mg, 0.4725 mmol) in MeOH (40 mL) was added $Mn^{II}(py)_4(SCN)_2$ (230 mg, 0.4723 mmol) as a solid, causing an immediate colour change to pale orange. The solution was stirred under Ar for 4 hours and then exposed to air which caused an immediate colour change to dark brown. After exposure to air for 7 days a dark red-brown precipitate was observed. The resulting dark red-brown solid was collected by filtration and dried *in vacuo* (185 mg, 78%). (Found: C, 53.18; H, 4.76; N, 16.73; S, 12.42%. Calc. for $[C_{22}H_{23}N_6S_2Mn\bullet 0.5H_2O]$ (499.53 g mol^{-1}): C, 52.90; H, 4.84; N, 16.82; S, 12.84%). IR (ATR): ν/cm^{-1} = 3393, 3235, 2948, 2039, 1611, 1555, 1541, 1456, 1434, 1399, 1353, 1298, 1248, 1229, 1204, 1156, 1139, 1127, 1110, 1087, 1071, 1057, 1039, 989, 976, 954, 940, 886, 857, 782, 756, 734, 641, 606, 591, 552, 480, 468, 448, 434, 409. ESI(+) MS (*m*/*z*) (MeCN): $[Mn^{III}\mathbf{L}^{Pr}\text{-}H]^+$ expected 373.1185, found 373.1219. μ_{eff} (SQUID at 300 K) = 4.91 μ_B. UV-vis (MeCN): λ_{max}/nm (ε/dm^3 mol^{-1} cm^{-1}) = 315 (10884), 478 (5093), 550 (1472), 872 (309). Λ_m (MeCN) = 36 Ω^{-1} cm^2 mol^{-1}. X-ray quality crystals were grown by slow evaporation of the reaction solution, giving red blocks of $[Mn^{III}\mathbf{L}^{Pr}(NCS)_2]$.

$[Mn^{IV}{}_2\mathbf{L}^{Et}{}_2(O)_2](ClO_4)_2\bullet 3.6H_2O$: In air, to a bright yellow solution of $H\mathbf{L}^{Et}$ (90.4 mg, 0.309 mmol) in a 1:1 mixture of methanol and dichloromethane (40 mL) was added manganese(II)perchlorate hexahydrate (112.0 mg, 0.309 mmol) as a solution in methanol (3 mL) resulting in a dark brown solution. A solution of triethylamine (31.1 mg, 0.309 mmol) was added resulting in no further colour change. This dark brown solution was stirred at RT overnight and concentrated to 20 mL by blowing compressed air over it and subjected to diethyl ether vapour diffusion. The dark brown solid was collected, dried *in vacuo*, then left in air (65 mg, 21%). Found: C, 44.12; H, 4.24; N, 10.95%. Calc. for $[C_{36}H_{38}N_8Cl_2O_{10}Mn_2\bullet 3.6H_2O$ (988.38 g mol^{-1}): C, 43.75; H, 4.61; N, 11.34%. IR (ATR): ν/cm^{-1} = 3504, 3293, 2946, 1628, 1596, 1559, 1541, 1458, 1436, 1395, 1281, 1195, 1163, 1084, 972, 912, 875, 852, 810, 755, 649, 621, 593, 562, 538, 492, 457. ESI(+) MS (*m*/*z*) (MeCN): $[Mn^{II}\mathbf{L}^{Et}\text{-}H]^+$ expected 345.0895, found 345.0906 $[Mn^{IV}{}_2\mathbf{L}^{Et}{}_2(O)_2(ClO_4)]^+$ expected 823.1349, found 823.1358. μ_{eff} (PPMS at 300 K) = 3.91 μ_B. UV-vis (MeCN): λ_{max}/nm (ε/dm^3 mol^{-1} cm^{-1}) = 374 (8222), 485 (3529). A few single crystals, suitable for an X-ray structure determination, were obtained by diethyl ether vapour diffusion into a DMF solution of the sample, giving dark brown needles of $[Mn^{IV}{}_2\mathbf{L}^{Et}{}_2(O)_2](ClO_4)_2\bullet 3DMF$.

X-ray Crystallography

Data were collected on a Bruker Kappa Apex II area detector diffractometer at 89-90 K using graphite monochromated Mo-Kα radiation (λ = 0.71073 Å). Both data sets (Tables S1 and S2, SI) were absorption corrected using SCALE. The structures were

solved using SHELXS-97 and refined against F^2 using all data by full-matrix least-squares techniques with SHELXL-97. All non-hydrogen atoms were modelled anisotropically except where noted. Hydrogen atoms were inserted at calculated positions and rode on the atoms to which they are attached except where noted. Crystallographic data has been deposited with the Cambridge Crystallographic Data Centre (reference numbers CCDC 1913017-1913018).

$[Mn^{III}L^{Pr}(NCS)_2]$: The asymmetric unit contains two $[Mn^{III}L^{Pr}(NCS)_2]$ complexes. The Mn(2) complex has no disorder, whereas in the Mn(1) complex both the thiocyanate anions have the CS atoms disordered over two sites with 0.75:0.25 occupancy whilst the N atom is full occupancy. The alkyl carbon atoms adjacent to the N atoms in the dipropylene triamine chain and the NH proton are disordered with 0.75:0.25 occupancy. The NH and the central C in each propylene chain are full occupancy. All non-hydrogen atoms were refined anisotropically except for the 0.75 and 0.25 occupancy C and N atoms of the dipropylene triamine chain and the 0.75 and 0.25 occupancy C and S atoms of the thiocyanate anion which were left isotropic.

$[Mn^{IV}_2L^{Et}_2(O)_2](ClO_4)_2$•3DMF: The asymmetric unit comprised the entire macrocyclic dimeric complex, two perchlorates anions and three DMF molecules of solvation. No disorder was present in the complex. One of the perchlorate anions was disordered over two sites with 0.8:0.2 occupancy. One of the DMF molecule was disordered over two sites with 0.7:0.3 occupancy. All non-hydrogen atoms were refined anisotropically except for the 0.2 occupancy perchlorate anion atoms, Cl25, O25, O26, O27 and O28. The 0.3 occupancy DMF atoms, C75, O75, N75, C76 and C77 were also refined isotropically.

Acknowledgements

This work was supported by grants from the University of Otago (including a PhD scholarship for RKW) and the MacDiarmid Institute for Advanced Materials and Nanotechnology (including a PhD scholarship for SD). We are grateful for access to the EPSRC UK National EPR Facility.

Conflicts of interest

There are no conflicts to declare.

References

(1) Lindoy, L. F., *The Chemistry of Macrocyclic Ligand Complexes*. Cambridge University Press: Cambridge, 1990.
(2) Gerbeleu, N. V.; Arion, V. B.; Burgess, J., *Template Synthesis of Macrocyclic Compounds*. Wiley-VCH: Weinheim, 1999.
(3) Messerschmidt, A.; Huber, R.; Poulos, T.; Wieghardt, K., *Handbook of Metalloproteins*. John Wiley and Sons, Ltd: Chichester, 2001; Vol. Vol 1.
(4) Smith, K. M., *Porphyrins and Metalloporphyrins*. Elsevier/North-Holland Biomedical Press: New York, 1976.
(5) Scott, A. I., Biosynthesis of vitamin B12. In search of the porphyrin-corrin connection. *Acc. Chem. Res.*, **1978**, *11*, 29-36.
(6) Larson, E. J.; Pecoraro, V. L., *Manganese Redox Enzymes*. VCH: New York, 1992; p 1-28.
(7) Barynin, V. V.; Whittaker, M. M.; Antonyuk, S. V.; Lamzin, V. S.; Harrison, P. M.; Artymiuk, P. J.; Whittaker, J. W., Crystal structure of manganese catalase from Lactobacillus plantarum. *Structure*, **2001**, *9*, 725-738.
(8) Gerasimchuk, N. N.; Gerges, A.; Clifford, T.; Danby, A.; Bowman-James, K., Dimanganese(II) accordion porphyrin as a functional model for catalases. *Inorg. Chem.*, **1999**, *38*, 5633-5636.
(9) Lingappa, U. F.; Monteverde, D. R.; Magyar, J. S.; Valentine, J. S.; Fischer, W. W., How manganese empowered life with dioxygen (and vice versa). *Free Radical Biology and Medicine*, **2019**.
(10) Costa, R. O.; Ferreira, S. S.; Pereira, C. A.; Harmer, J. R.; Noble, C. J.; Schenk, G.; Franco, R. W. A.; Resende, J. A. L. C.; Comba, P.; Roberts, A. E.; Fernandes, C.; Horn Jr., A., A New Mixed-Valence Mn(II)Mn(III) Compound With Catalase and Superoxide Dismutase Activities. *Frontiers in Chemistry*, **2018**, *6*.
(11) Britt, R. D.; Suess, D. L. M.; Stich, T. A., An Mn(V)–oxo role in splitting water? *Proc. Natl. Acad. Sci. U.S.A.*, **2015**, *112*, 5265-5266.
(12) Yano, J.; Yachandra, V., Mn4Ca Cluster in Photosynthesis: Where and How Water is Oxidized to Dioxygen. *Chem. Rev.*, **2014**, *114*, 4175-4205.
(13) Tsui, E. Y.; Kanady, J. S.; Agapie, T., Synthetic Cluster Models of Biological and Heterogeneous Manganese Catalysts for O2 Evolution. *Inorg. Chem.*, **2013**, *52*, 13833-13848.
(14) Ledesma, G. N.; Eury, H.; Anxolabéhère-Mallart, E.; Hureau, C.; Signorella, S. R., A new mononuclear manganese(III) complex of an unsymmetrical hexadentate N3O3 ligand exhibiting superoxide dismutase and catalase-like activity: synthesis, characterization, properties and kinetics studies. *J. Inorg. Biochem.*, **2015**, *146*, 69-76.
(15) Lee, W.-T.; Muñoz III, S. B.; Dickie, D. A.; Smith, J. M., Ligand Modification Transforms a Catalase Mimic into a Water Oxidation Catalyst. *Angew. Chem. Int. Ed.*, **2014**, *53*, 9856-9859.
(16) Ferreira, K. N.; Iverson, T. M.; Maghlaoui, K.; Barber, J.; Iwata, S., Architecture of the photosynthetic oxygen-evolving center. *Science (Washington D.C.)*, **2004**, *303*, 1831-1838.
(17) Mukhopadhyay, S.; Mandal, S. K.; Bhaduri, S.; Armstrong, W. H., Manganese clusters with relevance to Photosystem II. *Chem. Rev.*, **2004**, *104*, 3981-4026.
(18) Glerup, J.; Goodson, P. A.; Hazell, A.; Hazell, R.; Hodgson, D. J.; McKenzie, C. J.; Michelsen, K.; Rychlewska, U.; Toftlund, H., Synthesis and Characterization of Bis(μ-oxo)dimanganese(III,III), -(III,IV), and -(IV,IV) Complexes with Ligands Related to N,N'-Bis(2-pyridylmethyl)-1,2-ethanediamine (Bispicen). *Inorg. Chem.*, **1994**, *33*, 4105-4111.
(19) Philouze, C.; Blondin, G.; Girerd, J.-J.; Guilhem, J.; Pascard, C.; Lexa, D., Aqueous Chemistry of High-Valent Manganese. Structure, Magnetic, and Redox Properties of a New Type of Mn-Oxo Cluster, $[Mn^{IV4}O_6(bpy)_6]^{4+}$: Relevance to the Oxygen Evolving Center in Plants. *J. Am. Chem. Soc.*, **1994**, *116*, 8557-8565.
(20) Pal, S.; Armstrong, W. H., Products from reactions of manganese oxo complex $[Mn_2O_2(O_2CCH_3)(tpen)]^{2+}$ in acidic and neutral aqueous media: $[Mn_2(\mu\text{-}O)_2(\mu\text{-}O_2CCH_3)(tpen)]^{3+}$ and $[\{Mn_3(\mu\text{-}O)_4(OH)(tpen)\}_2(\mu\text{-}tpen)]^{6+}$. *Inorg. Chem.*, **1992**, *31*, 5417-23.
(21) Mukhopadhyay, S.; Staples, R. J.; Armstrong, W. H., Toward synthetic models for high oxidation state forms of the Photosystem II active site metal cluster: the first tetranuclear manganese cluster containing a $[Mn_4(u\text{-}O)_5]^{6+}$ core. *Chem. Commun.*, **2002**, 864-865.
(22) Koumousi, E. S.; Mukherjee, S.; Beavers, C. M.; Teat, S. J.; Christou, G.; Stamatatos, T. C., Towards models of the oxygen-evolving complex (OEC) of photosystem II: a Mn4Ca cluster of relevance to low oxidation states of the OEC. *Chem. Commun.*, **2011**, *47*, 11128-11130.
(23) Hocking, R. K.; Brimblecombe, R.; Chang, L.-Y.; Singh, A.; Cheah, M. H.; Glover, C.; Casey, W. H.; Spiccia, L., Water-oxidation catalysis by manganese in a geochemical-like cycle. *Nat. Chem.*, **2011**, *3*, 461-466.
(24) Yagi, M.; Toda, M.; Yamada, S.; Yamazaki, H., An artificial model of photosynthetic photosystem II: visible-light-derived O2 production from water by a di-l-oxo-bridged manganese dimer as an oxygen evolving center. *Chem. Commun.*, **2010**, *46*, 8594-8596.
(25) Brooker, S.; McKee, V.; Shepard, W. B.; Pannell, L. K., Formation of a (4+4) Schiff-base macrocyclic ligand by a template rearrangement, Crystal and molecular structure of two tetranuclear manganese(II) complexes. *J. Chem. Soc., Dalton Trans.*, **1987**, 2555-2562.
(26) Wieghardt, K.; Bossek, U.; Gebert, W., Synthesis of a Tetranuclear Manganese(IV) Cluster with Adamantane Skeleton: $[(C_6H_{15}N_3)_4Mn_4O_6]^{4+}$. *Angew. Chem. Int. Ed.*, **1983**, *22*, 328-329.
(27) McKee, V., Macrocyclic Complexes as Models for Nonporphine Metalloproteins. *Adv. Inorg. Chem.*, **1993**, *40*, 323-399.
(28) Curtis, N. F.; House, D. A., Structure of some aliphatic Schiff base complexes of nickel(II) and copper(II). *Chem. Ind.*, **1961**, 1708-1709.

(29) Curtis, N. F., The advent of macrocyclic chemistry. *Supramol. Chem.*, **2012**, *24*, 439–447.
(30) Pilkington, N. H.; Robson, R., Complexes of binucleating ligands III. Novel complexes of a macrocyclic binucleating ligand. *Aust. J. Chem.*, **1970**, *23*, 2225-2236.
(31) Sanyal, R.; Cameron, S. A.; Brooker, S., Synthesis and complexes of an N_4 Schiff-base macrocycle derived from 2,2'-iminobisbenzaldehyde. *Dalton Trans.*, **2011**, *40*, 12277-12287.
(32) Wilson, R. K.; Brooker, S., Complexes of a porphyrin-like N_4-donor Schiff-base macrocycle. *Dalton Trans.*, **2013**, *42*, 7913-7923.
(33) Wilson, R. K.; Brooker, S., Oxidative dehydrogenation of a new tetra-amine N_4–donor macrocycle tunes the nickel(II) spin state from high spin to low spin. *Dalton Trans.*, **2013**, *42*, 12075-12078.
(34) Black, D. S. C.; Rothnie, N. E., Metal template reactions. XIX. Macrocyclic metal complexes derived from 2,2'-iminobisbenzaldehyde and some primary diamines with additional nitrogen donor atoms. *Aust. J. Chem.*, **1983**, *36*, 2395-2406.
(35) Małecki, J. G.; Machura, B.; Świtlicka, A.; Groń, T.; Bałanda, M., Thiocyanate manganese(II) complexes with pyridine and its derivatives ligands. *Polyhedron*, **2011**, *30*, 746-753.
(36) Krzystek, J.; Telser, J.; Pardi, L. A.; Goldberg, D. P.; Hoffman, B. M.; Brunel, L.-C., High-Frequency and -Field Electron Paramagnetic Resonance of High-Spin Manganese(III) in Porphyrinic Complexes. *Inorg. Chem.*, **1999**, *38*, 6121-6129.
(37) Aromí, G.; Telser, J.; Ozarowski, A.; Brunel, L.-C.; Stoeckli-Evans, H.-M.; Krzystek, J., Synthesis, Crystal Structure, and High-Precision High-Frequency and -Field Electron Paramagnetic Resonance Investigation of a Manganese(III) Complex: [Mn(dbm)2(py)2](ClO4). *Inorg. Chem.*, **2005**, *44*, 187-196.
(38) Duboc, C.; Ganyushin, D.; Sivalingam, K.; Collomb, M.-N.; Neese, F., Systematic Theoretical Study of the Zero-Field Splitting in Coordination Complexes of Mn(III). Density Functional Theory versus Multireference Wave Function Approaches. *J. Phys. Chem. A*, **2010**, *114*, 10750-10758.
(39) Stebler, M.; Ludi, A.; Bürgi, H. B., Tetrakis(phenanthroline)di-.mu.-oxodimanganese(III,IV) tris(hexafluorophosphate).acetonitrile and tetrakis(phenanthroline)di-µ-oxodimanganese(IV) tetraperchlorate.acetonitrile: crystal structure analyses at 100 K, interpretation of disorder, and optical, magnetic, and electrochemical results. *Inorg. Chem.*, **1986**, *25*, 4743-4750.
(40) Goodson, P. A.; Glerup, J.; Hodgson, D. J.; Michelsen, K.; Pedersen, E., Binuclear Bis(µ-oxo)dimanganese(III,IV) and -(IV,IV) Complexes with N,N'-Bis(2-pyridylmethyl)-1,2-ethanediamine. *Inorg. Chem.*, **1990**, *29*, 503-508.
(41) Oki, A. R.; Glerup, J.; Hodgson, D. J., Syntheses and Characterization of Binuclear Manganese(III,IV) and -(IV,IV) Complexes with Ligands Related to Tris(2-pyridylmethyl)amine. *Inorg. Chem.*, **1990**, *29*, 2435-2441.
(42) Goodson, P. A.; Glerup, J.; Hodgson, D. J.; Michelsen, K.; Weihe, H., Syntheses and Characterization of Binuclear Manganese(III,IV) and -(IV,IV) Complexes with Ligands Related to *N,N*'-Bis(2-pyridylmethyl)-1,2-ethanediamine. *Inorg. Chem.*, **1991**, *30*, 4909-4914.
(43) Yatabe, T.; Kikkawa, M.; Matsumoto, T.; Nakai, H.; Kaneko, K.; Ogo, S., A model for the water-oxidation and recovery systems of the oxygen-evolving complex. *Dalton Trans.*, **2014**, *43*, 3063-3071.
(44) Goodson, P. A.; Hodgson, D. J., Synthesis and Characterization of a Bis(oxo)-Bridged $Mn^{III}Mn^{III}$ complex, Bis(µ-oxo)bis[N,N'-bis((6-methylpyrid-2-yl)methyl)ethane-1,2-diamine]dimanganese(III) Perchlorate. *Inorg. Chem.*, **1989**, *28*, 3606-3608.
(45) Brewer, K. J.; Calvin, M.; Lumpkin, R. S.; Otvos, J. W.; Spreer, L. O., Synthesis, Structure and Characterization of a Mixed-Valence Manganese (III)-Manganese (IV) Bis(µ-oxo) Complex with a Macrocyclic Tetraaza Ligand. *Inorg. Chem.*, **1989**, *28*, 4446-4451.
(46) Hanson, G. R.; Gates, K. E.; Noble, C. J.; Griffin, M.; Mitchell, A.; Benson, S., XSophe-Sophe-XeprView®. A computer simulation software suite (v. 1.1.3) for the analysis of continuous wave EPR spectra. *J. Inorg. Biochem.*, **2004**, *98*, 903-916.

Table of contents entry:

Monomeric and oxo-bridged dimeric manganese complexes of two flexible, anionic, [1+1] macrocycles, derived from diphenylamine-2,2'-dicarboxaldehyde and either diethyl- or dipropyl-enetriamine, are reported: both facial and meridional binding modes are observed.

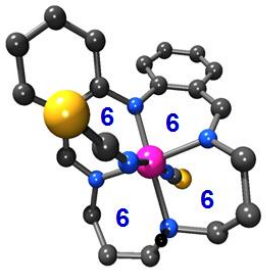

$[Mn^{III}L^{Pr}(NCS)_2]$

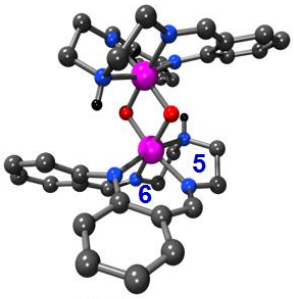

$[Mn^{IV}{}_2L^{Et}{}_2(O)_2](ClO_4)_2$